NIST GCR 00-795

Some Aspects of Fire Growth

James G. Quintiere
Department of Fire Protection Engineering
University of Maryland
College Park, MD 20742

NIST
National Institute of Standards and Technology
Technology Administration, U.S. Department of Commerce

NIST GCR 00-795

Some Aspects of Fire Growth

Prepared for
U.S. Department of Commerce
Building and Fire Research Laboratory
National Institute of Standards and Technology
Gaithersburg, MD 20899

By
James G. Quintiere
Department of Fire Protection Engineering
University of Maryland
College Park, MD 20742

August, 2000

U.S. Department of Commerce
Norman Y. Mineta, Secretary

Technology Administration
Dr. Cheryl L. Shavers, Under Secretary of Commerce for Technology

National Institute of Standards and Technology
Raymond G. Kammer, Director

Notice

This report was prepared for the Building and Fire Research Laboratory of the National Institute of Standards and Technology under Grant Number 60NANB6D0120. The statement and conclusions contained in this report are those of the authors and do not necessarily reflect the views of the National Institute of Standards and Technology or the Building and Fire Research Laboratory.

TABLE OF CONTENTS

Some Aspects of Fire Growth

James G. Quintiere
Department of Fire Protection Engineering
University of Maryland, College Park, MD 20742

ABSTRACT

A discussion of work is presented on the author's approach to develop predictions for fire growth phenomena. This approach has favored the development of approximate analytical formulas which convey the dominant mechanisms of the phenomena, and which have practical utility. The discussion includes the phenomena of ignition, burning rate, flame spread, flashover and fire plumes. Recent work on wood combustion, and a correlation for the near field entrainment in fire plumes is presented.

INTRODUCTION

Fire is a complex phenomena that defies simple mathematical expressions to portray all of its features. However, when these features are broken down into identifiable parts, a concept emerges that allows some simplified modeling. The translation of science into engineering applications follows this process. Today we see more of fire science being used to solve problems, and some engineers have hope of converting the fire safety regulation system into an engineering based design process, namely, performance based codes. In the current world of expanding computer capacities, it is very likely that the solution to problems based on the mathematical formulations of the 19th century will be solved by the computer in the 21th century. Yet, with still a 20th century mentality, it is safe to say that fire engineering is still resting on formulas and correlations. One might say that the use of predictive formulas has been the theme of 20th century engineering, and fire engineering lags the general field due to its complexity and its relative small amount of research.

My work has tended to focus on the formulation of solutions to aspects of fire phenomena in terms of formulas supported by modeling and by experimental results. The strategy has been toward the general, using the minimum amount of parameters sufficient to represent the dominant physics. Inspired by the success of others, I have tried to follow this philosophy. In applying formulas developed to predict fire phenomena, I have been amazed at their success in examples of demonstrating results to students in the

classroom, and in the investigation of features of accidents related to fire. The work of P. H. Thomas is rich in practical formulas for fire behavior [1]. One such formula given by Thomas has shown new students in fire engineering that the speed of flame spread through arrays of small sticks, randomly chosen and assembled by them, actually can be related to the bulk density of the wood in the array. The same formula was used to explain why it took 3 days for a fire to propagate about 100 m in a buried strata of tree stumps and branches. Although formulas are not easily validated on this scale, their level of consistency gives them added credibility. We have been encouraged by the success in the extrapolation of small sample oven data using the theory of spontaneous ignition of solids to confirm or establish the fire accident scenario involving stored materials [2]. Another interesting application used the small scale developed equations of Fay and Lewis [3] on the behavior of fire balls. This case was a fire investigation which supported the source of a large fireball, 22 m diameter and 49 m high, as a ruptured tank containing about 40 kg of propane. The generality and practical application of formulas to fire phenomena are invaluable, and still need more development and consensus to fully be appreciated.

One area that is still very weak, is the application of formulas to describe the fire behavior of materials. It is difficult to establish general formulations to represent the many features of real materials and products. Thus, the evaluation of the fire hazard of materials has been based in a wide array of empirical testing found in regulatory practices today. There is not a uniquely acceptable technical consensus on how to approach this problem. Over the last decade, we have investigated the feasibility of using the minimum amount of parameters in the formulation of analytical formulas to evaluate the various aspects of material fire behavior, namely: ignition, burning rate, flame spread and fire growth. Each material fire process contributes new essential mechanisms, and therefore new properties that are needed in the formula. These properties, although modelling based, must have some universality or they are merely fitting parameters. The real answer for these "equivalent material properties" lies somewhere between meaningful science and mathematical coefficients.

For material properties to be practical in fire modeling they must not only produce accurate predictions, but they must be unambiguously deduced from test data. Keeping the number of properties to a minimum is also desirable. Since ignition precedes flame spread and burning, its properties feed into the latter two processes. The hierarchy of material properties with phenomena is shown in Table 1, and the relationship between phenomena and properties is

implied by "x". We shall discuss these relationships and their basis in formulas for the processes. I will draw on work done by students to whom I am deeply grateful.

Table 1. Material properties and Fire Process

PROCESSES / PROPERTIES	Igni-tion	Flame Spread	Burning Rate, Non-charring	Burning Rate, Char-ring
Ignition, Vaporization Temperature	x	x	x	x
Thermal Properties, original material	x	x	x	x
Heat of Gasification	--	--	x	x
Char Properties	--	--	--	x
Flame Heat Flux, Length	--	x	x	x

IGNITION

The simplest model for *piloted ignition* that can be rendered is that based purely on heat conduction. We shall consider the case of a *thermally thick solid* exposed to a constant incident heat flux, $\dot{q}_i''$, under convective and radiative cooling to a fixed temperature ambient at T_∞. Assumptions of the model include:

1. inert semi-infinite solid with constant thermal properties, kρc,
2. constant ignition temperature, T_{ig}, and
3. blackbody surface conditions.

Assumption 1 requires a minimal effect of energy sinks due to phase change and pyrolysis processes. To the extent these energy effects are important, they would be absorbed into an *effective kρc property*. Assumption 2 requires the same evolution of fuel gases at T_{ig} to always cause the lower flammable limit to occur at the pilot ignition source in a small time. Ideally, the time for pyrolysis must be very fast along with the time for mixing between the gaseous fuel and the air. Pyrolysis kinetics may play a significant role at low heat flux conditions near the critical flux for ignition, $\dot{q}_{cr}''$.

Since this problem is non-linear due to the radiation boundary condition, an exact analytical solution is not possible. An approximate integral solution yields the following dimensionless analytical solution for the time to ignite[4]:

$$\tau_{ig} = C\left(\frac{\dot{q}''_{cr}}{\dot{q}''_i}\right)^2 \tag{1}$$

$$\text{where } \tau_{ig} = \left(\frac{\dot{q}''_{cr}}{T_{ig} - T_\infty}\right)^2 \frac{t_{ig}}{k\rho c} \tag{1a}$$

$$\dot{q}''_{cr} = \sigma\left(T_{ig}^4 - T_\infty^4\right) + h_c\left(T_{ig} - T_\infty\right) \tag{1b}$$

$$\text{and } C = \frac{\pi/2}{(2-\beta)(1-\beta)},\ \beta = \frac{\dot{q}''_{cr}}{\dot{q}''_i}. \tag{1c}$$

The coefficient, C, was modified here by replacing 4/3 of the integral solution with $\pi/2$ so as to match the exact solution for purely convective heat loss. The exact solution for purely convective heat loss is

$$\frac{\dot{q}''_{cr}}{\dot{q}''_i} = 1 - e^{\tau_{ig}}\operatorname{erfc}\sqrt{\tau_{ig}} \to 2\sqrt{\tau_{ig}/\pi} \text{ as } \tau_{ig} \text{ becomes small.} \tag{2}$$

For the high flux limit, or correspondingly for small time limit, both Eqns (1) and (2) give the well known limit where C is $\pi/2$. An approximate solution to this non-linear problem has also been given, for the purely radiative heat loss case, by Delichatsios et al. [5]. Their asymptotic results are

$$\frac{1}{\sqrt{\tau_{ig}}} = \sqrt{\pi}\left(\frac{\dot{q}''_i}{\dot{q}''_{cr}} - 1\right), \text{ for } \frac{\dot{q}''_i}{\dot{q}''_{cr}} \le 1.1 \tag{3a}$$

$$\frac{1}{\sqrt{\tau_{ig}}} = \frac{2}{\sqrt{\pi}}\left(\frac{\dot{q}''_i}{\dot{q}''_{cr}} - 0.64\right), \text{ for } \frac{\dot{q}''_i}{\dot{q}''_{cr}} \ge 3.0. \tag{3b}$$

Eq. (1) can also be put in the same form as Eq (3b) for $\dot{q}''_i / \dot{q}''_{cr} \ge 2$ with the intercept of 0.64 replaced by 0.76, and for Eq. (2) the intercept replaced as

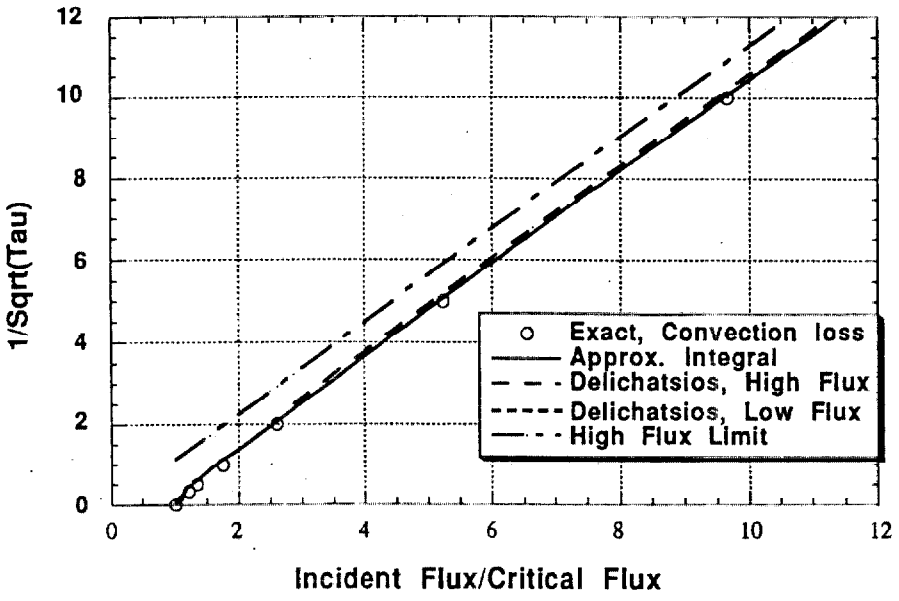

Figure 1. Comparison of Ignition Solutions

0.80. Figure 1 shows a comparison of these solutions, and demonstrates the accuracy of Eq. (1). The more simple limit solution with C as $\pi/2$ under-predicts the dimensionless time as the dimensionless heat flux decreases toward 1. The limit solution might give an acceptable estimate for $\dot{q}_i'' / \dot{q}_\alpha'' \geq 2$ where $t_{ig,limit}/t_{ig}$ ranges from about 0.5 to 1.

Any of these equations offers a means for comparing experimental data. They can also be used to fit experimental data by appropriately selecting the material properties: $k\rho c$ and T_{ig}. However, there can be operational difficulties in implementing this property derivation since the simple conduction theory may not always apply. In other words, these two properties may be insufficient since other factors such as pyrolysis or oxidation of the solid may increase in importance and their mechanisms may not be neglected. This, of course, is the limitation of a purely conductive model for ignition. Nevertheless, such a model does capture the first order effects and can be applied to a host of materials with good success. A plot of the ignition data in the form of $t_{ig}^{-1/2}$ versus $\dot{q}_i''$ offers a means to determine the critical heat flux from the intercept on the x-axis by using Eq. (3b), T_{ig} from Eq. (1b), and $k\rho c$ from the slope of the graph. Since the slope depends on

$(T_{ig}-T_\infty)\sqrt{k\rho c}$, any inaccuracy in determining $\dot{q}''_{cr}$ affects T_{ig} and therefore $k\rho c$, accordingly.

Table 2 shows some derived ignition properties. One always is tempted to examine the thermal (inertia) property and the ignition temperature as derived in this empirical way with directly measured values. In general, it is typical that the $k\rho c$ value found in this way is higher than the directly measured value at normal temperature, perhaps due to the variation of k and c with temperature. Also the ignition temperature is likely to be underestimated due to the difficulty in experimentally finding the critical heat flux for ignition, which can be attributable to not having the patience to wait long enough for ignition at low heat fluxes. The extrapolation method suggested by Eq (3) to find the critical flux from "an intercept" is only likely to work for materials where conduction is the dominant mechanism for ignition. For example, the limitation of Eq.(3) in this regard, is evident when the intercept yields a negative value, which is common as shown in Figure 2. On the other hand, Figure 3 gives an example of a dimensionless plot of ignition data for a variety of wood species. The tightness of the data to a linear fit following the simple conduction theory shows the appropriateness of the derived properties and the theory.

A curious aspect of the set of ignition data shown in Figure 3 is that it involves ignition times as long as 1 hour or more at incident heat fluxes of as low as 5 kW/m^2. At these conditions, spot glowing was observed on the surface of the wood, indicating the presence of oxidation. The apparent augmentation of the supplied heat flux by the energy from the wood oxidation is clearly indicated in the change of the slope for the low heat flux data of Figure 4.

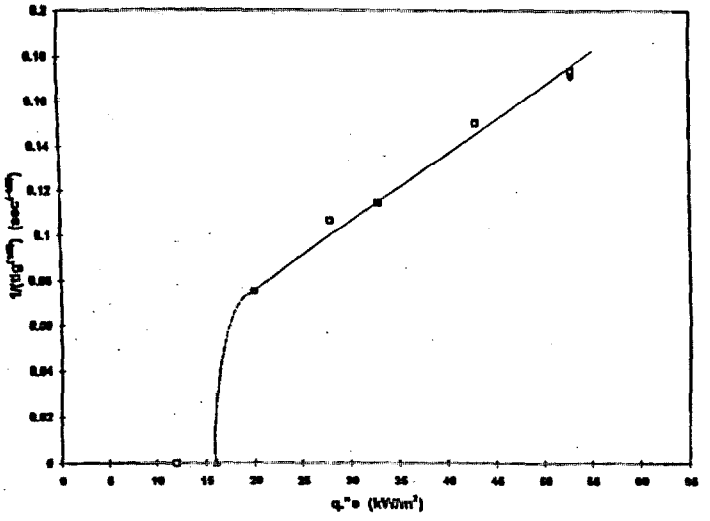

Figure 2. $t_{ig}^{-1/2}$ versus $\dot{q}''_i$ for wood fiberboard [5]

Table 2. Derived Material Properties [4,8]

Material	ρ kg/m^3	T_{ig} °C	$k\rho c$ kJ^{2}m^{-4}K^{-2}s^{-1}	Δh_c kJ/g	L kJ/g$_{lost}$	L_o kJ/g$_{orig}$	Char Frac. ϕ -	Cone Flame Heat Flux kW/m^2
Redwood,L*	354	375	0.22	11.9	9.4	2.83	0.12-0.41	35
Redwood, X*	328	204	2.07	9.0	7.5	3.18	0.17-0.45	33
Douglas fir,L	502	384	0.25	11.0	12.5	1.57	0.27-0.62	17
Douglas fir,X	455	258	1.44	9.1	6.8	2.93	0.16-0.42	46
Red oak,L	753	304	1.01	12.3	10.0	2.34	0.21-0.49	35
Red oak,X	678	275	1.88	12.1	4.5	2.33	0.00-0.39	33
Maple,L	741	354	0.67	13.0	4.4	1.70	0.41-0.71	16
Maple,X	742	150	11.0	12.1	6.3	3.53	0.06-0.39	36
PMMA(Polycast)	1190	180+	2.1	--	2.8	2.8	0	37
Nylon	1169	380+	0.87	--	3.8	3.8	0	30
Polyethylene	955	300+	1.8	--	3.6	3.6	0	25
Polypropylene	900	210+	2.2	--	3.1	3.1	0	14

*L, cut along the grain; X, cut across the grain; +, underestimated.

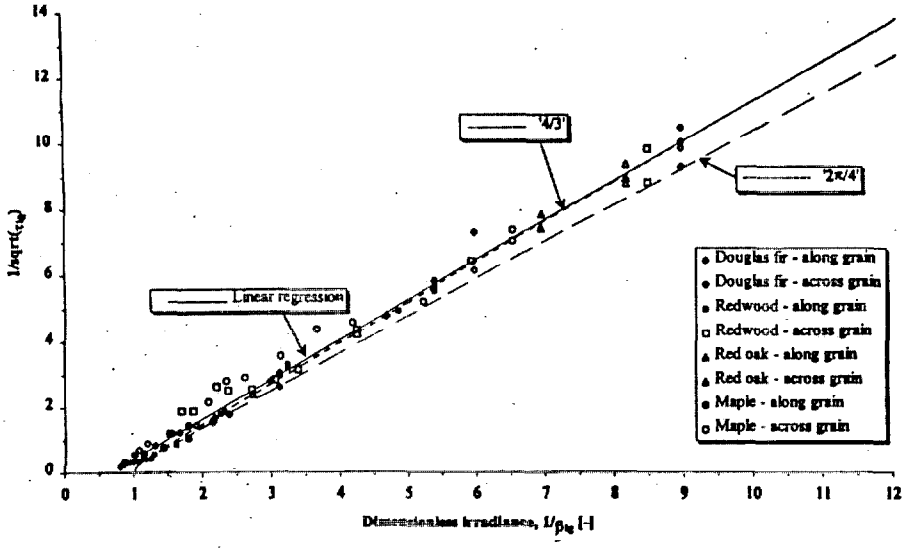

Figure 3. Ignition correlation based on Eq.(3) for wood species [4]

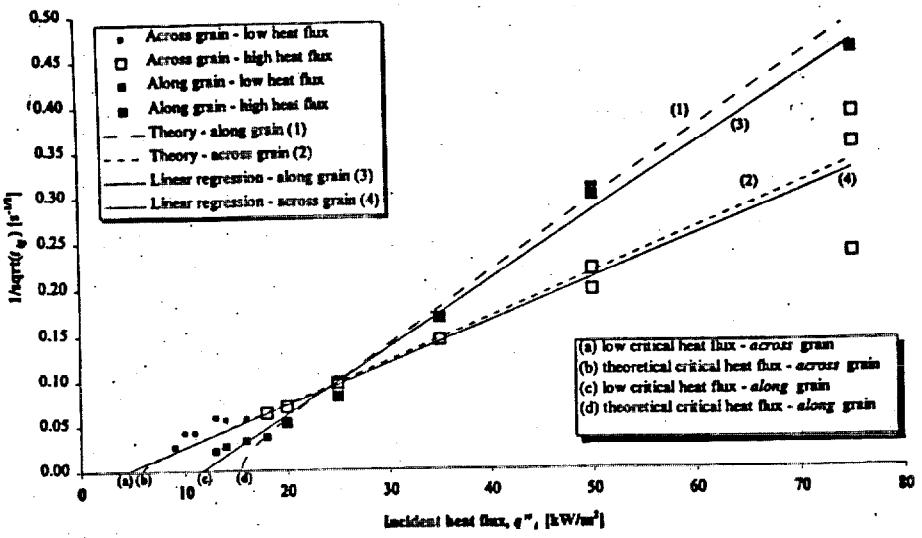

Figure 4. Low heat flux ignition of redwood [4]

BURNING RATE

The simplest model to represent the mass loss rate of a solid due to an incident heat flux is to consider it as a steady state evaporating liquid at an original temperature, T_∞. For this idealization, the mass loss rate per unit area, $\dot{m}''$, is given in terms of the net heat flux, $\dot{q}''$, as

$$\dot{m}'' = \dot{q}''/L \qquad (4)$$

where L is the heat of gasification given as the sum of the heat of vaporization, ΔH_v, and the sensible energy needed to bring the solid fuel from its original temperature to its vaporization temperature, T_v, i.e.

$$L=\Delta H_v+c(T_v-T_\infty). \qquad (5)$$

As long as the solid fuel will vaporize without leaving a char residue, there is relatively no ambiguity on how to define *L as a material property*. For a charring material, an appropriate definition for L in order to obtain mass *loss* rate might be taken as

$$L=L_o/(1-\phi) \text{ in kJ/g fuel lost} \qquad (6)$$

where L_o is based on the original mass of material as given by Eq. (5), and ϕ is

the char fraction. Table 2 gives some typical results for L and L_o, and shows the effect of the char fraction giving $L>L_o$ for a given polymer. These results are in conformity with the suggested relationship in Eq. (6). The property L for a charring material is very approximate since it must be based on some *defined burning rate* during its transient process, and then on how it varies with the incident heat flux. In Table 2, an average peak burning rate was selected. As we will see, the value L_o given in Table 2 for the wood materials was also determined by an empirical fit of the transient data, and is still a modeling parameter. But L_o has more precise physical meaning than L since it is the *energy required* to break the polymer bonds of the *original* material to yield char and gas. In contrast, L is a bulk property involving this pyrolysis energy, the char fraction, and depends on the *averaging* procedure used.

A solution which tries to take into account the transient burning behavior is more complex, especially for a charring material. A transient burning rate solution has been found from an approximate integral model based on studies we conducted [4,7-9] and is nearly identical to a formulation by Moghtaderi et al. [10]. The approximate solution has been shown to be in good agreement with more exact numerical solutions for the same equations. Therefore, the integral solution offers the prospect for analytical results which can more clearly display the importance of properties and variables. The specific transient burning rate problem considered is a *thermally thick* solid with a *constant incident heat flux* composed of external radiative and flame components. The problem addresses the initial preheating needed for ignition, and the potential development of a char layer. The significant modeling assumptions include:

1. the ignition temperature is the vaporization temperature,
2. the solid vaporizes at a fixed temperature with a constant heat of vaporization, ΔH_v,
3. the flame heat flux and the char fraction are constant, and
4. all thermal properties are constant.

The theoretical results will be compared to data from the Cone Calorimeter using 10 cm square horizontal samples. The Assumption 3 specifying a constant flame heat flux can be justified for this sample configuration if the sample energy release rate exceeds about 200 kW/m^2. This is supported by Rhodes et al. [8] in which a gas burner simulated-sample was used to measure the flame heat flux, and can also be supported by the emissivity of a homogeneous cylindrical flame becoming constant as the flame height exceeds about twice the base diameter. For shorter flames, especially in the decay period for charring materials, the assumption of constant flame heat flux in the

Cone Calorimeter will be weak.

Therefore, in our model, the net heat flux to the surface for the burning problem is given as

$$\dot{q}'' = \dot{q}''_{-} \equiv \dot{q}''_{i} - \sigma(T_{ig}^4 - T_\infty^4) - h_c(T_{ig} - T_\infty),\ t \le t_{ig} \qquad (7a)$$

$$\dot{q}'' = \dot{q}''_{+} \equiv \dot{q}''_{i} - \sigma(T_{ig}^4 - T_\infty^4) + \dot{q}''_{f},\ t \ge t_{ig} \qquad (7b)$$

where $\dot{q}''_f$ is the total flame heat flux. This step change in heat flux produces a step change in the mass loss rate in the model when combustion occurs. This modeling approximation produces an instantaneous burning rate when the flame appears, and is given as

$$\dot{m}''_{ig} = \frac{(1-\phi)}{\Delta H_v}\left(\dot{q}''_f + h_c(T_{ig} - T_\infty)\right). \qquad (8)$$

Non-Charring Result (ϕ=0)

The transient non-charring burning rate can be given as [7]:

$$\frac{\dot{m}''L}{(1-\phi)\dot{q}''_{+}} = \left(\frac{L}{\Delta H_v}\right)\left(1 - \frac{c(T_{ig} - T_\infty)}{L}\left(\frac{1}{\Delta}\right)\right) \qquad (9)$$

with

$$\frac{1-\Delta}{1-\Delta_{ig}} = \exp\left(-(\Delta - \Delta_{ig}) - 6\left(\frac{L}{\Delta H_v}\right)(\tau - \tau_{ig})\right)$$

where here $\tau \equiv \frac{\left(\frac{k}{\rho c}\right)t}{\delta_s^2}$ is a dimensionless time, and

$\delta_s \equiv \frac{2kL}{c\dot{q}''_{+}}$ is a thermal conduction length needed to achieve steady vaporization.

Δ is a dimensionless thermal length, δ/δ_s, and Δ_{ig} is its value at ignition.

At steady state Δ=1, and the left-hand-side of Eq. (9) is also equal to 1. For typical solids, a representative value for δ_s is about 1 cm with a corresponding time to reach steady burning of about 1 minute (based on k=0.2 W/m-K, c=2 kJ/kg-K, ρ=500 kg/m^3, L=3 kJ/g and ΔH_v=1.5 kJ/g). Table 2 gives the values of L for several non-charring plastics derived from steady state data indicative of Figure 5. In addition to the ignition derived properties, information is also

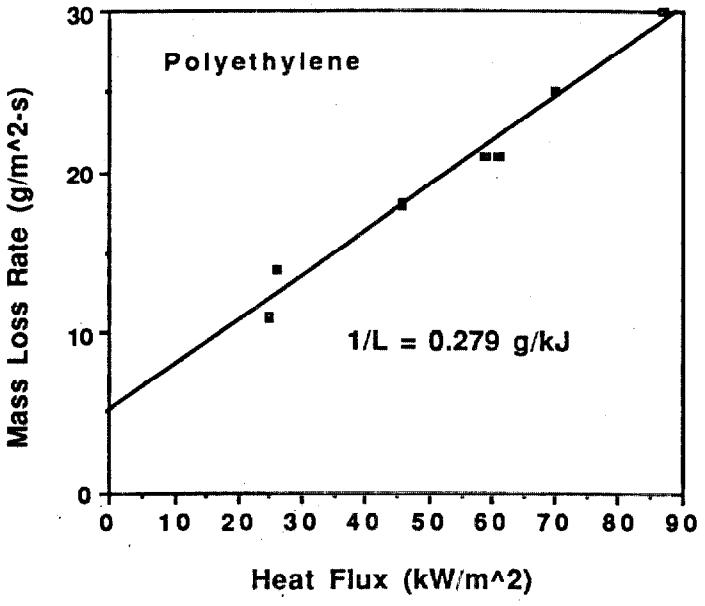

Figure 5. Steady burning rate for Polyethylene with incident heat flux [9]

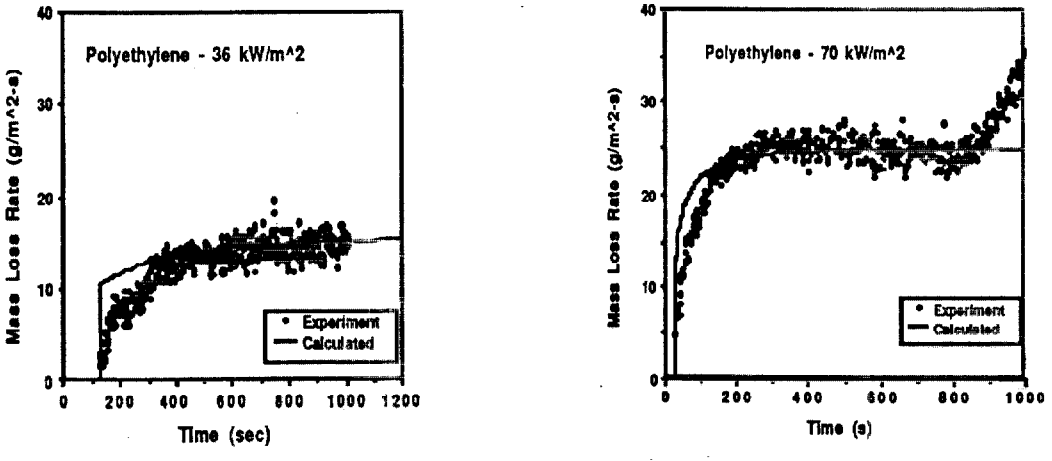

(a) (b)

Figure 6. Transient burning rate for Polyethylene[9]

needed on specific heat and this was selected from the literature. Figures 6a and 6b show typical predictions of transient burning compared to measured data in the Cone Calorimeter. Table 2 also gives needed corresponding values for the flame heat flux in the Cone heater for horizontal burning. The flame heat flux can be determined from Eqns. (4) and (7b) and the data in Figure 5.

Charring Result

The corresponding equations that arise from an approximate integral solution are highly nonlinear, and an analytical solution is not directly possible. However,approximate analytical solutions can be produced for small and large times, and their combination produce reasonable results. The solutions are summarized below:

Small Time: The small time charring result follows the non-charring case with a given ϕ up to a peak burning rate after which the long time solution begins. The short time burning rate solution is given from Eq. (9) as

$$\frac{\dot{m}'' L_o}{(1-\phi)\dot{q}''_+} = \left(\frac{L_o}{\Delta H_v}\right)\left(1 - \frac{c(T_{ig}-T_\infty)}{L_o}\left(\frac{1}{\Delta}\right)\right) \qquad (10)$$

$$\text{where } \Delta \approx \Delta_{ig} + 6\left(\frac{L_o}{\Delta H_v}\right)\left(1-\Delta_{ig}\right)\left(\tau - \tau_{ig}\right).$$

It can be shown that the char depth is initially linear in time and in heat flux:

$$\delta_c \approx \frac{\dot{q}''_f}{\rho \Delta H_v}\left(1 - \frac{\dot{q}''_-}{\dot{q}''_+}\right)\left(t - t_{ig}\right). \qquad (11)$$

The surface temperature, $T_s \approx T_{ig}$.

Large Time: The long time solution is given as follows:

$$\delta_c \approx \sqrt{\frac{2k_c(T_s - T_{ig})(t - t_{ig})}{\rho \Delta H_v}} \qquad (12)$$

$$\dot{m}'' = (1-\phi)\rho \frac{d\delta_c}{dt} \approx (1-\phi)\sqrt{\frac{\rho k_c (T_s - T_{ig})}{2\Delta H_v (t - t_{ig})}}, \qquad (13)$$

$$\delta \approx \left[\left(\frac{2k(T_v - T_\infty)}{\dot{q}''_-}\right)^2 + 12\left(\frac{k}{\rho c}(t - t_{ig})\right)\right]^{1/2} \qquad (14)$$

and

$$T_s \approx \frac{\left(\dot{q}''_f + \dot{q}''_i\right)^{1/4}}{\sigma}. \qquad (15)$$

The additional property needed for the charring solution is k_c, the char conductivity which can be estimated as ϕk [4]. The serious property limitation is the determination of L_o and the char fraction ϕ, as well as the empirical determination of the flame heat flux. Values for some wood species are shown in Table 2. The char fraction was measured and empirically was found to inversely vary with the incident heat flux. L_o and the flame heat flux were determined selected to give the "best" overall fit between data and the analytical theory. This process was tedious and attempted to use dimensionless variables as a guide.

A sample of the typical results obtained in comparing the theory to charring data is displayed in Figure 7 for Douglas fir cut along the grain at an incident heat flux of 50 kW/m^2 (directed perpendicular to the wood grain). The theoretical results reasonably following the behavior of the measured burning rate. The sudden rise to a peak burning rate is very rapid, and the decay is inversely related to the square root of time. For long times, the burning rate is very weakly affected by incident heat flux and generally approaches a value of the order of 5 g/m^2-s. Consequently, the actual variability in flame heat flux does not strongly affect this result.

It was empirically found by Spearpoint [4] for wood samples that the *fictitious* steady mass burning rate for a charring material given by Eqns. (4) and (6) is related to its actual peak burning rate, as

$$\dot{m}''_{peak} = \gamma(1-\phi)L_o / \dot{q}''_+ \qquad (16)$$

with γ decreasing from about 1 to 0.4 while the char fraction decreases from about 0.5 to 0.2 as the incident heat flux is correspondingly increased from 25 to 75 kW/m2.

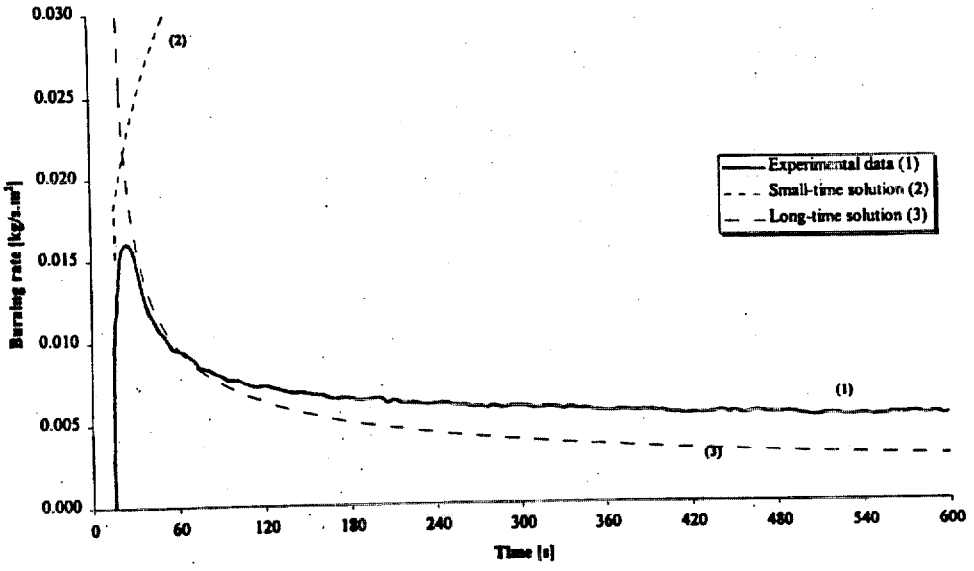

Figure 7. Burn Rate for Douglas fir at 50 kW/m2 [4]

Figure 8 shows the corresponding thermal penetration depth (δ) compared to an imbedded thermocouple increase of 5° C. The thermal depth does not exceed the thickness of the wood over the time shown, and in general the 50 mm sample remains thermally thick for at least 10 to 15 minutes.

The char depth for the same Douglas fir test is displayed in Figure 9 for 22 minutes. The experimental results were determined by three different methods: (1) the numerical integration of Eq. (13) using the burning rate data, (2) an imbedded thermocouple reaching the ignition temperature (384° C for Douglas fir), and (3) the thermocouple reaching a generic char temperature of 288° C.

The thermocouple originally at 4 mm from the surface was taken to represent the quasi-steady surface temperature after long time (about 20 min.) and compared to the approximate result in Eq. (15). Results are shown in Figure 10 for Douglas fir with the theory offering some credibility depending on the flame heat flux assigned, roughly 0, 17 or 46 kW/m2.

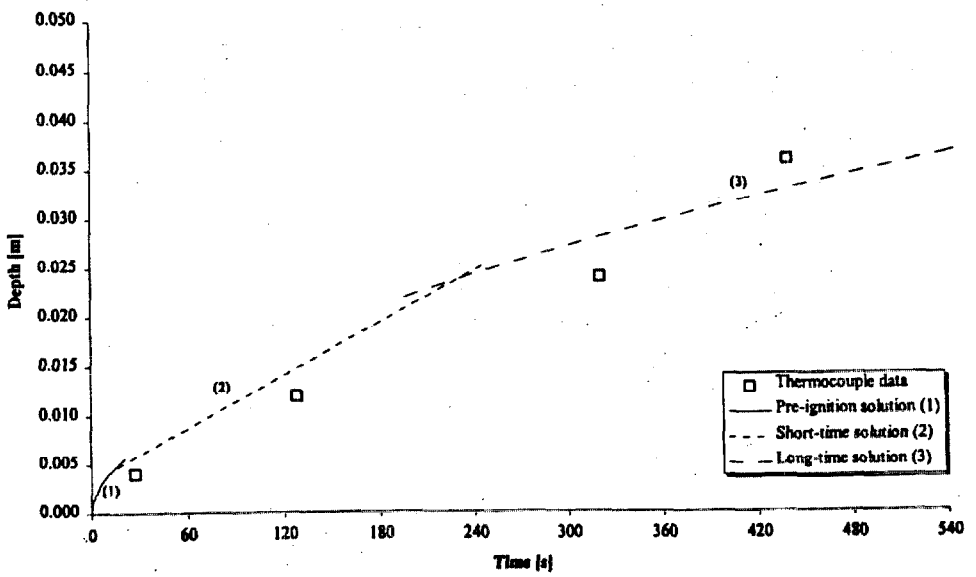

Figure 8. Thermal depth, Douglas fir [4]

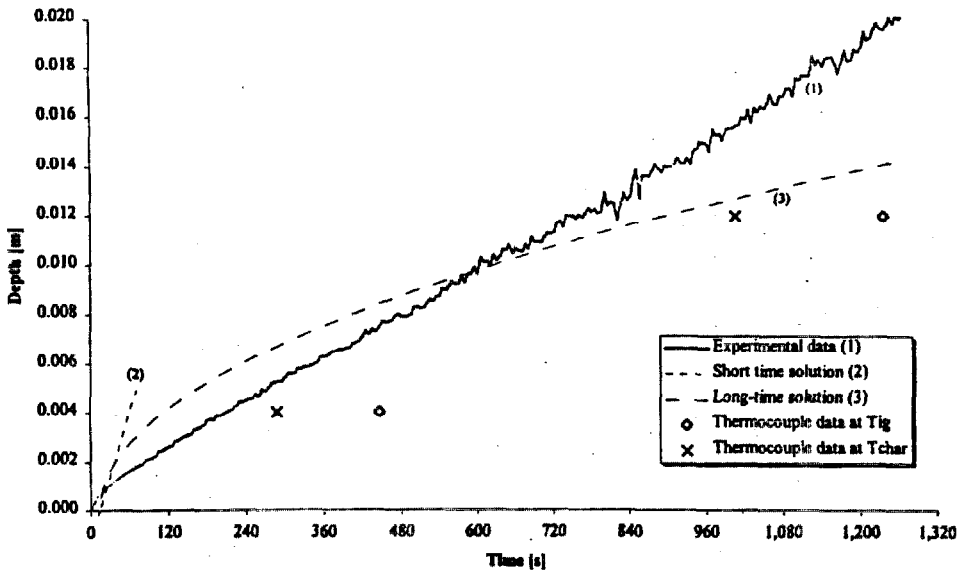

Figure 9. Char depth, Douglas fir [4]

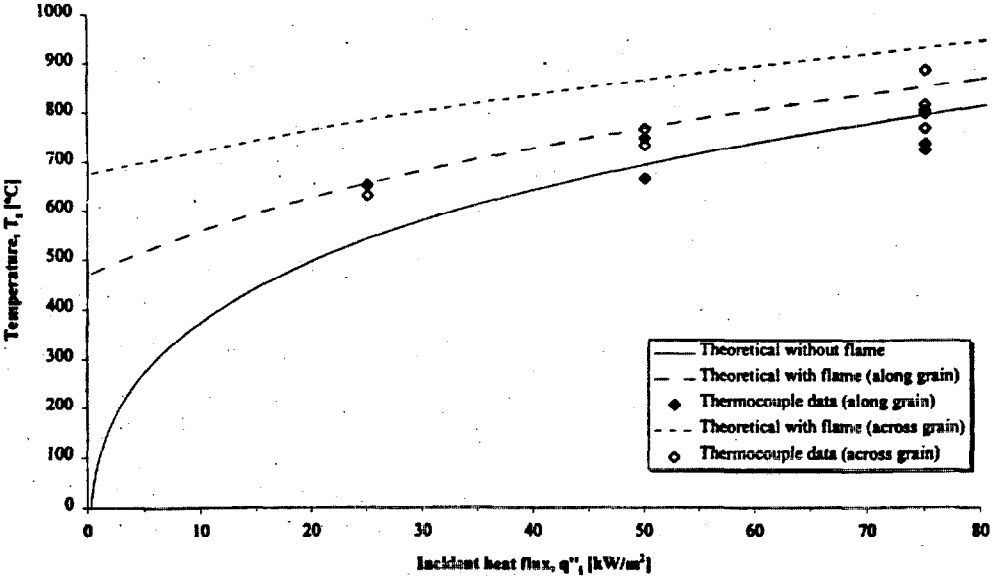

Figure 10. Surface Temperature for Douglas fir [4]

FLAME SPREAD AND FIRE GROWTH

There is a relationship between flame spread and ignition. These two phenomena are complementary; one begins where the other leaves off. This can be seen from the "flammability diagram" in Figure 11. Here the material is a (thermally) thin plastic film on an insulating fiberglass substrate, and is exposed to a uniform incident radiant heat flux. The data show the results of piloted ignition from a fixed ambient temperature and upward flame spread velocity based on the material at a equilibrium surface temperature based on the incident heat flux. It can be shown that both the time to ignite and the velocity data have a vertical asymptote at the critical heat flux for ignition which is about 24 kW/m^2 in this case. These data were taken with the plastic film thermally bonded to the substrate. If the material were not bonded, on heating it would rip and roll away. This would typically eliminate the possibility of ignition or flame spread. The rip-data are also shown , and together this "diagram" might be used to explain the flammability characteristics of a material, especially since heat flux plays such a critical role in the disposition of fire hazard for a material

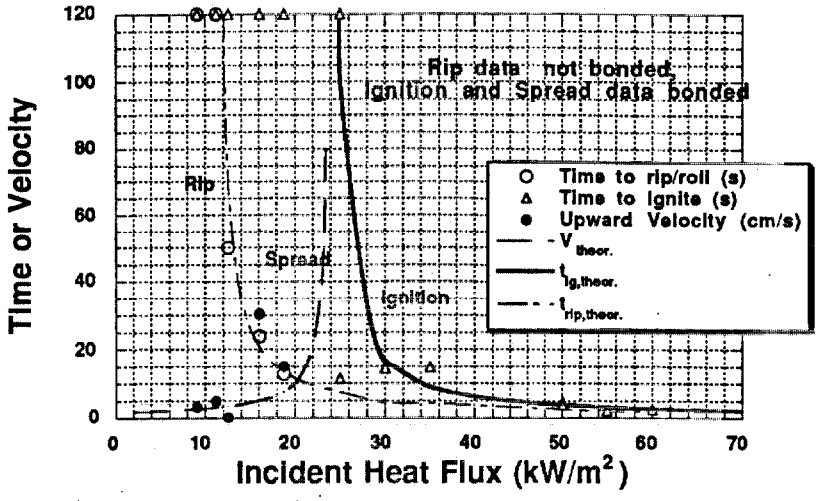

Figure 11. Flammability diagram of a thin plastic film

The simplest basis to develop an expression for the flame spread speed, V, on a surface is

$$V = \frac{\text{Heated Distance}}{\text{Ignition Time}} \qquad (17)$$

For *upward flame spread*, if the "heated length" is equated with the flame extension ahead of the pyrolysis zone, and that length is assumed linearly related to the energy release rate of the material, then an expression for flame speed can be developed. This leads to an accelerating characteristic with a dimensionless parameter, b, determining the magnitude and sign of the acceleration. This model can also incorporate the consumption of a material by a burning time, t_b. Such a model has been described by Cleary and Quintiere [11]. The parameter b can be expressed as

$$b = (0.01 m^2 kW)\dot{m}'' \Delta h_c - 1 - t_{ig}/t_b \qquad (18)$$

where the burning rate and burning time can be computed from Eq. (4) and the ignition time from Eq. (1), all based on the flame heat flux. The properties come from the type assembled in Table 2.

The fire hazard on wall and ceiling material can be primarily viewed as an upward flame spread problem which can be driven by the initial heat flux characteristics of the source fire. This scenario is very much representive of the ISO 9705 Room-Corner Test. The flame spread parameter given in Eq. (18) will be a critical factor in establishing the time to reach *flashover* in this room test. Since flashover in a given room can be associated with a fixed energy release rate, the time to reach this critical value will be related to b. Kim and Quintiere [12], using a simulation model [13], found for a range of material properties, that the dimensionless flashover time (t_{FO}/t_{ig}) is an inverse function of b with the vertical asymptote shifting to the left as the dimensionless burning time ($\tau_b=t_b/t_{ig}$) decreases. The critical b value to just cause flashover appears to slightly decrease as a material becomes thinner. The theoretical results are shown in Figure 12, and Figure 13 shows the corresponding experimental results for 45 materials. These materials included construction products composed of wood, plastics, and composites mostly represented by painted or paper covered gypsum board. The similarity between the modeling and experimental correlations is good, and both the simulation model and the experimental plot have been based on the simple modeling equations described in this paper and on their associated properties as exemplified by Table 2.

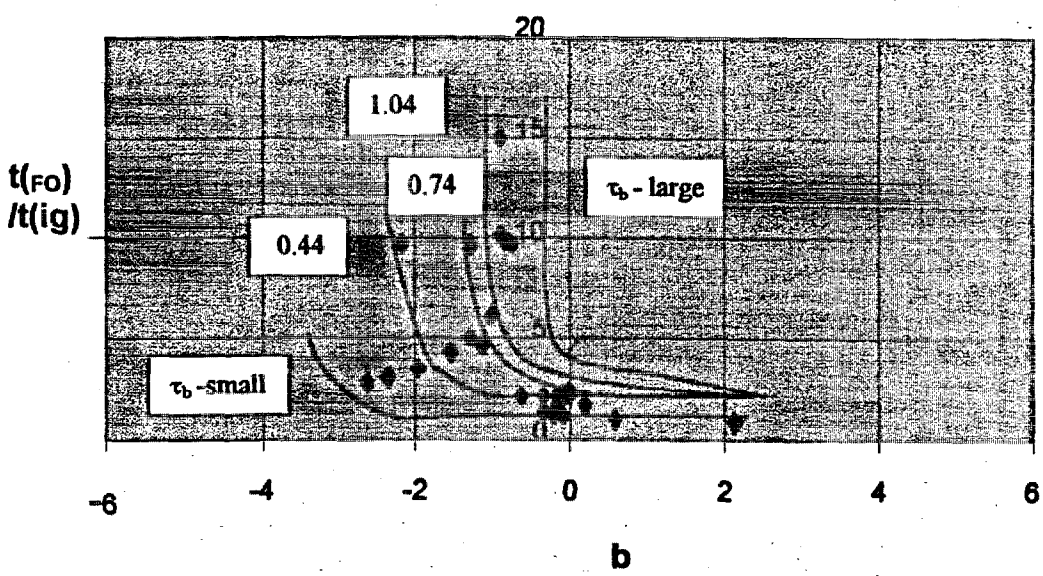

Figure 12. ISO 9705 Flashover correlation from computations [12]

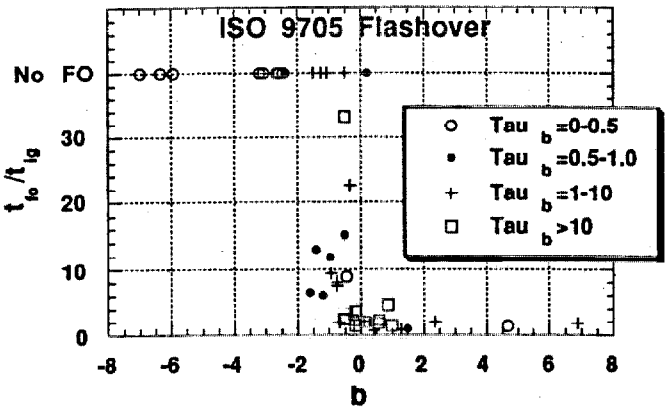

Figure 13. ISO 9705 Flashover correlation from experiments [14]

FIRE PLUMES

Turbulent fire plumes preclude fundamental computational results and rely on approximate methods supported by data to yield useful correlations. Many significant studies have been done, and some observations will be made. The observations are based on an analysis which attempted to unify and review various data sources on plumes of different base geometries [15]. The analysis followed a Boussinesq model using gaussian profiles and a uniform flame radiative fraction, X_r. The "best" fit of the approximate solutions led to some new correlations and values for modeling parameters that might give some insight into the processes. Some interesting findings are listed below.

1. There is a relationship that holds between the plume centerline velocity, w, and temperature rise, $T-T_\infty$, at height z which suggests nearly a direct relationship between kinetic energy and potential energy. From inviscid flow theory it can be shown for a constant pressure plume that

$$\frac{w^2}{\left(\frac{T-T_\infty}{T_\infty}\right)gz} = 2. \qquad (19)$$

Based on data for both axisymmetric plumes of diameter D and line fires of width D and length L, the constant in Eq. (19) is found to be 1.5±0.1 for the

entire region of the plumes including the combustion region. This is a remarkably similar result.

2. The gaussian entrainment coefficient was found to be 0.098 and 0.091 for the axisymmetric and line plumes outside the combustion regions. It was higher in the combustion regions with line plume being about 2.5 times that of the circular geometry. This suggests a similar mixing mechanism in the far-field and some enhanced mixing mechanism near the base of a line fire.

3. There is an intimate relationship between the flame length and the flame entrainment rate. It was found that both the circular and line fires exhibited 9.6 times stoichiometric air required in the combustion region suggesting a similarity for the turbulent combustion process.

4. Some illustrative new correlations are shown for the flame entrainment rate into a circular fire, and for flame length from a line fire in Figures 14 and 15 respectively. The correlations include the effect of fuel type and flame radiation in the parameter

$$\Psi = \frac{(1 - X_r)\Delta h_c / s}{c_p T_\infty} \qquad (20)$$

where X_r is the radiation fraction,

Δh_c is the heat of combustion, and

s is the stoichiometric mass air to fuel ratio.

This correlation for flame entrainment rate smoothly takes into account the dependence on diameter D, and shows that flame entrainment does not depend on the energy release rate of the fire. The correlation for flame length does depend on energy release rate in terms of the parameters

$$Z^{**} = \left(\frac{\dot{Q}/L}{\rho_\infty c_p T_\infty g^{1/2}} \right)^{2/3}, \quad Q_D^{**} = \left(\frac{Z^{**}}{D} \right)^{3/2}. \qquad (21)$$

The line fire flame length correlation in Figure 15 shows a curious bifurcation of the data which is not explained, but may be related to the methodology used to define the fluctuating flame length.

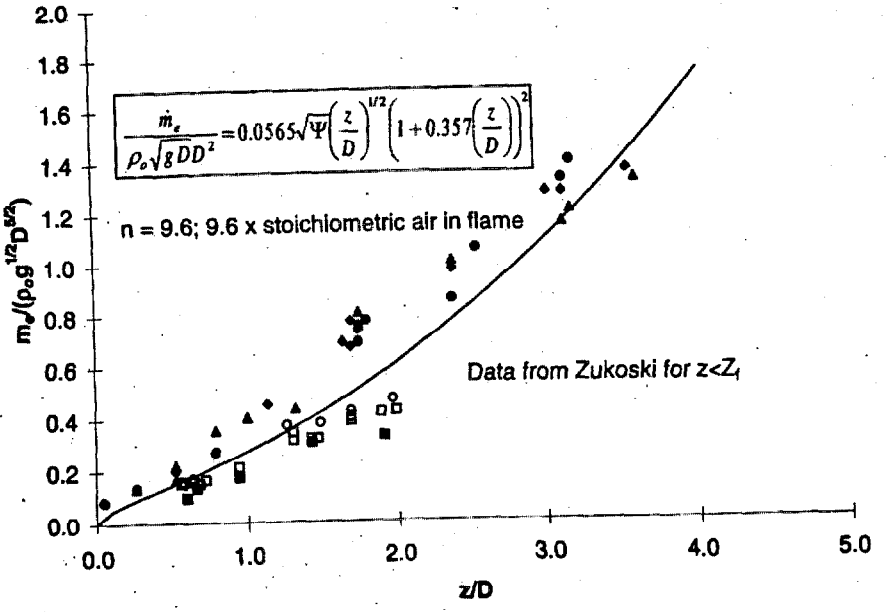

Figure 14. Axisymmetric flame entrainment rate, X_r=0.3, D=0.19,0.50 m [15]

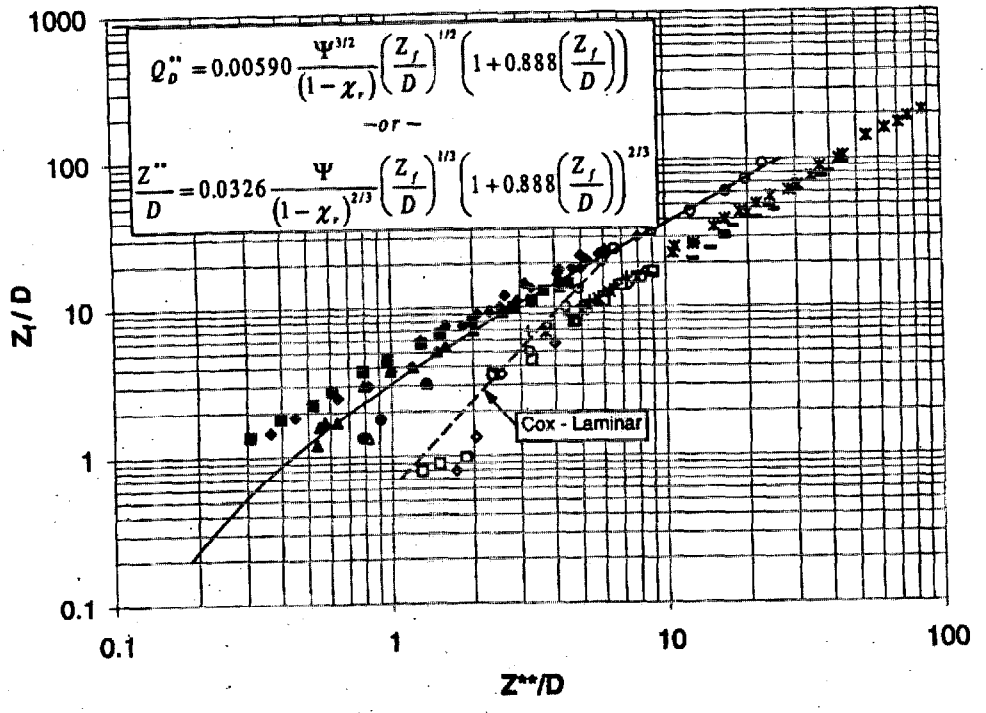

Figure 15. Line flame length, data from various sources [15]

SUMMARY

A discussion has been presented to illustrate the development and use of simplified formulas to describe fire processes. Modeling properties and parameters have been used to link analytical relationships with data. There has been an attempt to retain the essential physics and to enhance the generality of the modeling parameters. Hopefully the examples discussed will give a balanced impression of the success of the formulas presented.

NOMENCLATURE

b	parameter defined in Eq. (19)
c_p	specific heat
D	diameter, width
g	acceleration due to gravity
h	convective heat transfer coefficient
k	thermal conductivity
L	heat of gasification
m	mass
q	heat
Q	energy release
t	time
T	temperature
V	flame speed
w	vertical velocity
z	position
ρ	density
τ	dimensionless time, Eq. (1) or (9)
Δh_c	heat of combustion

Subscripts

b	burn-out
ig	ignition
s	surface
∞	ambient

Superscripts

$\dot{()}$	per unit time

REFERENCES

1. P. H. Thomas, "Fire Research Station 1951-1986 Selected Papers", Building Research Estab., Dept. Environ., Garston, UK, 1986.

2. Hill, S. and Quintiere, J. G., Case Studies in Spontaneous Ignition, *Fire and Materials*, accepted for pub., 1999.

3. Fay, J. and Lewis, D. H., 16th Intl. Symp. on Comb., The Combustion Institute, Pittsburgh, PA, 1976, p. 1387.

4. Spearpoint, J.M.,"Predicting the Ignition and Burning Rate of Wood in the Cone Calorimeter Using an Integral Model", NIST-GCR-99-977, Nat. Inst. Stand. Tech., Gaithersburg, MD, April 1999.

5. Delichatsios, M. A., Panagiotou, T-H, Kiley, F., *Combustion and Flame*, **84**, 1991, p. 323.

6. Dillon, S. E., Kim, WH, Quintiere J. G., "Determination of Properties and the Prediction of the Energy Release Rate of Materials in the ISO 9705 Room-Corner Test", NITST-GCR-98-754, Nat. Inst. Stand. Tech., Gaithersburg, MD, June 1998.

7. Quintiere, J. and Iqbal, N., *Fire and Materials*, **18**, 1994, p. 89.

8. Rhodes, B. T. and Quintiere, J. G., *Fire Safety Journal*, **26**,3, 1996, p. 221.

9. Hopkins, D.,Jr. and Quintiere, J. G., *Fire Safety Journal*, **26**,3, 1996, p. 241.

10. Moghtaderi, B. Novozhilov, V., Fletcher, D. Kent, J.H., *Fire and Materials*, **21**, 1997, p. 7.

11. Cleary, T. G. And Quintiere, J. G., "A Framework for Utilizing Fire Property Tests", *Fire Safety Sci. Proc. 3rd Int. Symp.*, ed. G. Cox and B. Langford, Elsevier Appl. Sci., London, 1991, p. 674.

12. Kim, W H and Quintiere, J. G., " Applications of a Model to Compare Flame Spread and Heat Release Properties of Interior Finish Material in a Compartment", Int. Symp. Fire Sci. Tech. , Seoul, Korea, Nov. 12-14, 1997.

13. Quintiere, J. G. *Fire Safety Jour.*, **20**, 4, 1993, p. 313.

14. Dillon, S. E., Quintiere, J. G., Kim, W.H., "Discussion of a Model and Correlation for the ISO Room-Corner Test", *Sixth Int. Symp. Fire Safety Sci.*, Poitiers, France, July 5-9, 1999.

15. Quintiere, J. G. and Grove, B. S., "A Unified Analysis for Fire Plumes", 27th Symp. Int. on Combustion, The Combustion Inst. Pittsgburgh, PA, 1998, p.2757.

FLASHOVER TIME
ISO9705 Room Corner Test

For a given room fire, $t_{FO}/t_{ig} \propto 1/b$

$$b = (0.01 m^2 kW) \dot{m}'' \Delta h_c - 1 - t_{ig}/t_b$$

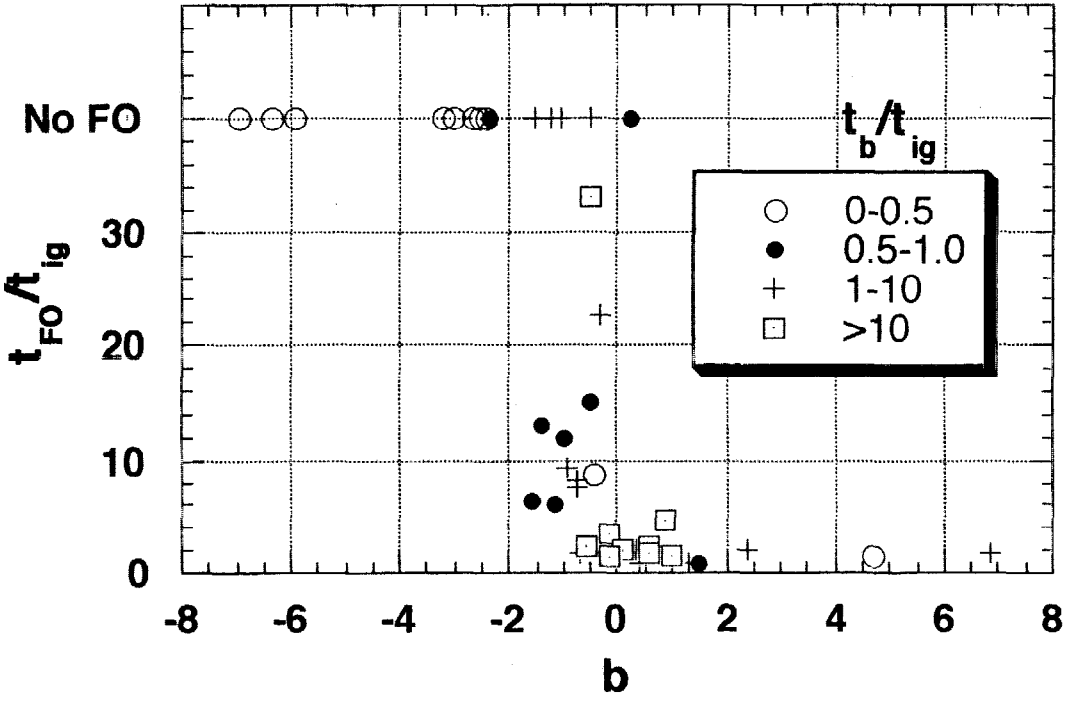

Table 1. Material Fire Properties

Materials Grouped according to Type	Tig (°C)	Ta,min (°C)	kρc (kW²s / m⁴K²)	Φ (kW² / m³)	$\Delta Hc_{peak\ avg}$ (kJ / g)	$L_{peak\ avg}$ (kJ / g)	Q''_{total} (MJ / m²)
COMPOSITES							
S4 Gypsum Board	469	380	0.515	14	7	4.8	2.8
R402 Paper Faced Gypsum Board	515	517	0.549	0.0	6.4	4.8	2.2
S6 Paper Wall Covering on Gypsum Board	388	300	0.593	0.5	10	4.8	7.2
8-E Surface Treatment on Gypsum board	516	398	0.562	3.2	20.08	3.48	3.8
8-F F.R. Surface Treatment on Gypsum board	516	273	0.694	20.1	16.07	6.44	5.9
7-Ao PVC Wall Paper (300 g/m²) on Gypsum board	507	422	0.226	1.7	11.03	3.39	3.5
8-L PVC Wall Paper (800 g/m²) on Gypsum board	394	300	0.453	7.0	12.70	4.00	8.1
E10 PVC Wallcarpet on Gypsum Board	391	367	0.69	8.2	6.5	3.3	11.0
S5 PVC Covering on Gypsum Board	410	300	0.208	25	13	3.7	4.6
8-B Rayon Wall Paper (300 g/m²) on Gypsum board	394	217	0.843	24.4	17.06	7.34	6.7
S7 Textile Covering on Gypsum Board	406	270	0.570	9	13	1.5	8.3
E3 Textile Covering on Gypsum Board	387	189	0.97	7.7	7.5	3.1	9.5
8-C Emulsion Paint on Gypsum board	649	594	0.462	14.2	17.84	2.08	3.4
8-D Acrylic Enamel on Gypsum board	560	292	0.419	26.2	14.97	5.12	4.0
E1 Painted Gypsum Paper on Plaster Board	551	478	0.73	3.3	4.1	3.6	3.3
S8 Textile Covering on Mineral Wool	391	174	0.183	6	25	2.8	9.3
E5 Plastic faced Steel Sheet on Mineral Wool	582	472	0.60	44	11.0	34.0	2.5
E7 Combustible faced Mineral Wool	354	263	0.11	0.86	11.0	9.2	1.7
PLASTICS PRODUCTS							
R407 F.R. PVC	415	352	1.306	0.2	9.9	10.4	16.1
S10 Expanded Polystyrene (PS)	482	130	0.464	31	28	1.5	32.0
R420 F.R. Expanded Polystyrene Board (40 mm)	295	77	1.594	4.2	27.5	7.3	33.9
R421 F.R. Expanded Polystyrene Board (80 mm)	490	77	0.557	7.1	26.9	12.7	25.5
E11 Extruded Polystyrene Foam	482	354	0.44	11.5	27.0	2.7	20.0
R405 F.R. Extruded Polystyrene Board	275	77	1.983	1.2	27.8	4.7	38.7
S11 Polyurethane Foam (rigid)	393	105	0.031	3	13	3.1	14.0
R404 PU Foam Panel with Paper Facing	250	77	0.199	8.7	18.9	5.5	30.8
E9 Polyurethane Foam on Plastic faced Steel Sheet	494	326	0.60	22	12.0	5.1	17.0
R406 Clear Acrylic Glazing	195	195	2.957	—	24.1	1.6	89.5
8-H F.R. Polyethylene Foam on Metal Plate (Foam side tested)	593	498	0.713	43.5	57.02	12.93	3.8
R408 3-Layed F.R. Polycarbonate Panel	495	167	1.472	0.0	19.5	3.3	58.1
E4 Melamine faced High Density Non-Combustible Board	631	527	0.32	12.7	8.5	3.5	7.0
WOOD PRODUCTS							
R409 Varnished Massive Timber	330	77	0.530	6.9	16.3	17.5	68.2
S12 Wood Panel (Spruce)	389	155	0.569	24	15	6.3	120.0
R411 Normal Plywood	290	147	0.633	2.2	11.9	7.3	64.6
E2 Ordinary Birch Plywood	392	164	0.99	13	11.9	6.2	75.5
R410 F.R. Plywood	480	197	0.105	0.7	11.2	9.3	51.8
7-Q Soft Fiberboard	245	261	0.581	11.4	13.89	6.39	30.7
S2 Medium Density Fiberboard	361	80	0.732	11	14	4.2	100.0
S1 Insulating Fiberboard	381	90	0.229	14	14	4.2	68.0
R401 F.R.Chipboard	505	507	4.024	0.0	9.2	10.0	34.2
S3 Particle Board	405	180	0.626	8	14	5.4	120.0
S9 Melamine Covering on Particle Board	483	435	0.804	1	11	4.8	60.0
S13 Paper Covering on Particle Board	426	250	0.680	13	13	6.5	100.0
E8 F.R. Particle Board	678	678	1.80	—	6.0	4.0	6.0
E6 F.R. Particle Board Type B1	482	482	0.29	—	3.9	1.4	5.5

	Materials	t_{ig} (sec)	t_{fg} (sec)	t_b (sec)	τ_{ig} (—)	τ_b (—)	a (—)	b (—)
7-Ao	Gypsum board + PVC Wall Paper (300 g/m²)	610	47	28	13.04	0.59	0.27	-1.43
7-Q	Soft Fiberboard	54	26	253	2.10	9.84	0.22	0.11
8-B	Gypsum board + Rayon Wall Paper (300 g/m²)	672	103	59	6.53	0.57	0.13	-1.61
8-C	Gypsum Board + Emulsion Paint	∞	160	21	∞	0.13	0.63	-7.02
8-D	Gypsum board + Acrylic Enemel	∞	107	42	∞	0.39	-0.04	-2.59
8-E	Gypsum board + Surface Treatment	∞	121	17	∞	0.14	1.19	-5.77
8-F	Gypsum board + F.R. Surface Treatment	∞	149	62	∞	0.42	-0.05	-2.45
8-H	F.R. Polyethylene Foam on Metal Plate (Foam side tested)	∞	204	31	∞	0.15	0.24	-6.42
8-L	Gypsum board + PVC Wall Paper (800 g/m²)	834	55	52	15.08	0.95	0.55	-0.51
R401	F.R.Chipboard	∞	826	948	∞	4.05	-0.64	-1.51
R402	Paper Faced Gypsum Board	∞	117	43	∞	1.28	-0.49	-3.21
R403	PU Foam Panel with Aluminum Facing (room test)	41	9	—	17.72	—	0.92	0.86
R404	PU Foam Panel with Paper Facing (bench test)	—	—	161	—	69.51	—	—
R405	F.R. Extruded Polystyrene Board	96	113	119	3.38	4.19	2.25	1.30
R406	Clear Acrylic Glazing	141	79	104	7.12	5.24	7.63	6.87
R407	F.R. PVC	∞	178	343	∞	7.3	-0.55	-1.07
R408	3-Layed F.R. Polycarbonate Panel	∞	290	244	∞	3	1.38	0.19
R409	Varnished Massive Timber	107	44	1394	9.41	122.69	-0.51	-0.54
R410	F.R. Plywood	631	19	1029	117.44	191.58	-0.50	-0.52
R411	Normal Plywood	142	40	729	13.92	71.47	-0.11	-0.17
R420	F.R. Expanded Polystyrene Board (40 mm)	87	105	166	3.26	6.23	1.04	0.41
R421	F.R. Expanded Polystyrene Board (80 mm)	∞	107	290	∞	9.65	-0.14	-0.51
S1	Insulating Fiberboard	59	25	413	2.36	16.52	0.65	0.59
S2	Medium Density Fiberboard	131	72	590	1.82	8.2	0.69	0.57
S3	Particle Board	157	79	964	1.99	12.2	0.24	0.16
S4	Gypsum Board	∞	89	45	∞	0.5	-0.38	-2.35
S5	PVC Covered Gypsum Board	611	27	27	22.63	1.02	0.67	-0.3
S6	Paper Covered Gypsum Board	640	68	70	9.41	1.03	0.02	-0.95
S7	Textile Covered Gypsum Board	639	72	20	8.88	0.28	3.16	-0.46
S8	Textile Covered Mineral Wool	43	21	21	2.05	1.01	3.37	2.37
S9	Melamine Covered Particle Board	465	147	631	3.16	4.29	-0.05	-0.28
S10	Expanded Polystyrene (PS)	115	85	41	1.35	0.49	6.76	4.71
S11	Polyurethane Foam (rigid)	6	4	68	1.5	17.09	1.05	0.99
S12	Wood Panel (Spruce)	131	66	1026	1.98	15.55	0.17	0.11
S13	Paper Covered Particle Board	143	95	1076	1.51	11.33	-0.07	-0.16
E1	Painted Gypsum Paper Plaster Board	∞	176	86	∞	0.49	-0.61	-2.67
E2	Ordinary Birch Plywood	160	116	804	1.38	6.93	-0.06	-0.21
E3	Textile Covering on Gypsum Board	670	111	80	6.04	0.72	0.19	-1.2
E4	Melamine faced High Density Non-Combustible Board	∞	102	130	∞	1.28	-0.46	-1.25
E5	Plastic faced Steel Sheet on Mineral Wool	∞	162	260	∞	1.61	-0.9	-1.53
E6	F.R. Particle Board Type B1	630	53	47	11.89	0.9	0.16	-0.95
E7	Combustible faced Mineral Wool	75	10	28	7.5	2.77	-0.39	-0.76
E8	F.R. Particle Board	∞	669	294	∞	0.44	-0.8	-3.08
E9	Plastic faced Steel Sheet on Polyurethane Foam	215	115	179	1.87	1.56	-0.05	-0.69
E10	PVC Wallcarpet on Gypsum Board	650	81	114	8.02	1.41	-0.04	-0.74
E11	Extruded Polystyrene Foam	80	80	48	1	0.6	3.16	1.49

NIST-114
(REV. 11-94)
ADMAN 4.09

U.S. DEPARTMENT OF COMMERCE
NATIONAL INSTITUTE OF STANDARDS AND TECHNOLOGY

(ERB USE ONLY)
ERB CONTROL NUMBER | DIVISION
PUBLICATION REPORT NUMBER | CATEGORY CODE
PUBLICATION DATE | NUMBER PRINTED PAGES

MANUSCRIPT REVIEW AND APPROVAL

INSTRUCTIONS: ATTACH ORIGINAL OF THIS FORM TO ONE (1) COPY OF MANUSCRIPT AND SEND TO THE SECRETARY, APPROPRIATE EDITORIAL REVIEW BOARD.

TITLE AND SUBTITLE (CITE IN FULL)

Some Aspects of Fire Growth

CONTRACT OR GRANT NUMBER

60NANB6D0120

TYPE OF REPORT AND/OR PERIOD COVERED

Final Report - August, 2000

AUTHOR(S) (LAST NAME, FIRST INITIAL, SECOND INITIAL)

James G. Quintiere

PERFORMING ORGANIZATION (CHECK (X) ONE BLOCK)

- ☐ NIST/GAITHERSBURG
- ☐ NIST/BOULDER
- ☐ JILA/BOULDER

LABORATORY AND DIVISION NAMES (FIRST NIST AUTHOR ONLY)

SPONSORING ORGANIZATION NAME AND COMPLETE ADDRESS (STREET, CITY, STATE, ZIP)

Department of Commerce
National Institute of Standards and Technology, Gaithersburg, MD

PROPOSED FOR NIST PUBLICATION

- ☐ JOURNAL OF RESEARCH (NIST JRES)
- ☐ J. PHYS. & CHEM. REF. DATA (JPCRD)
- ☐ HANDBOOK (NIST HB)
- ☐ SPECIAL PUBLICATION (NIST SP)
- ☐ TECHNICAL NOTE (NIST TN)
- ☐ MONOGRAPH (NIST MN)
- ☐ NATL. STD. REF. DATA SERIES (NIST NSRDS)
- ☐ FEDERAL INF. PROCESS. STDS. (NIST FIPS)
- ☐ LIST OF PUBLICATIONS (NIST LP)
- ☐ NIST INTERAGENCY/INTERNAL REPORT (NISTIR)
- ☐ LETTER CIRCULAR
- ☐ BUILDING SCIENCE SERIES
- ☐ PRODUCT STANDARDS
- ☒ OTHER NIST GCR

PROPOSED FOR NON-NIST PUBLICATION (CITE FULLY) ☐ U.S. ☐ FOREIGN

PUBLISHING MEDIUM

- ☒ PAPER
- ☐ CD-ROM
- ☐ DISKETTE (SPECIFY)
- ☐ OTHER (SPECIFY)

SUPPLEMENTARY NOTES

ABSTRACT (A 2000-CHARACTER OR LESS FACTUAL SUMMARY OF MOST SIGNIFICANT INFORMATION. IF DOCUMENT INCLUDES A SIGNIFICANT BIBLIOGRAPHY OR LITERATURE SURVEY, CITE IT HERE. SPELL OUT ACRONYMS ON FIRST REFERENCE.) (CONTINUE ON SEPARATE PAGE, IF NECESSARY.)

A discussion of work is presented on the author's approach to develop predictions for fire growth phenomena. This approach has favored the development of approximately analytical formulas which convey the dominant mechanisms of the phenomena, and which have practical utility. The discussion includes the phenomena of ignition, burning rate, flame spread, flashover, and fire plumes. Recent work on wood combustion and a correlation for the near field entrainment in fire plumes is presented.

KEY WORDS (MAXIMUM OF 9; 28 CHARACTERS AND SPACES EACH; SEPARATE WITH SEMICOLONS; ALPHABETIC ORDER; CAPITALIZE ONLY PROPER NAMES)

burning rate, fire growth, fire plumes, flame spread, flashover

AVAILABILITY

- ☐ UNLIMITED
- ☐ FOR OFFICIAL DISTRIBUTION - DO NOT RELEASE TO NTIS
- ☐ ORDER FROM SUPERINTENDENT OF DOCUMENTS, U.S. GPO, WASHINGTON, DC 20402
- ☐ ORDER FROM NTIS, SPRINGFIELD, VA 22161

NOTE TO AUTHOR(S): IF YOU DO NOT WISH THIS MANUSCRIPT ANNOUNCED BEFORE PUBLICATION, PLEASE CHECK HERE. ☐

ELECTRONIC INFORMS